How to design quantum-jump trajectories via distinct master equation representations

Dariusz Chruściński[1], Kimmo Luoma[2,3], Jyrki Piilo[3], and Andrea Smirne[4,5]

[1]Institute of Physics, Faculty of Physics, Astronomy and Informatics, Nicolaus Copernicus University, Grudziadzka 5/7, 87-100 Toruń, Poland

[2]Institut für Theoretische Physik, Technische Universität Dresden, D-01062, Dresden, Germany

[3]Turku Center for Quantum Physics, Department of Physics and Astronomy, University of Turku, FI-20014, Turun Yliopisto, Finland

[4]Dipartimento di Fisica "Aldo Pontremoli", Università degli Studi di Milano, Via Celoria 16, I-20133 Milan, Italy

[5]Istituto Nazionale di Fisica Nucleare, Sezione di Milano, Via Celoria 16, I-20133 Milan, Italy

Every open-system dynamics can be associated to infinitely many stochastic pictures, called unravelings, which have proved to be extremely useful in several contexts, both from the conceptual and the practical point of view. Here, focusing on quantum-jump unravelings, we demonstrate that there exists inherent freedom in how to assign the terms of the underlying master equation to the deterministic and jump parts of the stochastic description, which leads to a number of qualitatively different unravelings. As relevant examples, we show that a fixed basis of post-jump states can be selected under some definite conditions, or that the deterministic evolution can be set by a chosen time-independent non-Hermitian Hamiltonian, even in the presence of external driving. Our approach relies on the definition of rate operators, whose positivity equips each unraveling with a continuous-measurement scheme and is related to a long known but so far not widely used property to classify quantum dynamics, known as dissipativity. Starting from formal mathematical concepts, our results allow us to get fundamental insights into open quantum system dynamics and to enrich their numerical simulations.

1 Introduction

Quantum jumps provide a powerful and insightful tool to describe the dynamics of open quantum systems [1, 2]. In the quantum-jump unraveling, the open-system state satisfying an assigned master equation is

Dariusz Chruściński: darch@fizyka.umk.pl
Kimmo Luoma: kimmo.luoma@tu-dresden.de
Jyrki Piilo: jyrki.piilo@utu.fi
Andrea Smirne: andrea.smirne@unimi.it

expressed as the average of – in principle, infinitely many – trajectories of pure states, which consist of deterministic evolutions interrupted by discontinuous, randomly distributed jumps [3]. Quantum jumps have been observed in several experimental platforms [4–9] and are computationally convenient to solve high-dimensional master equations, thus being routinely used to describe, e.g., quantum optical [10] or open many-body systems [11]. Interestingly, if the jumps are frequent and small enough, one can recover a different stochastic description of the open-system evolution, characterized by diffusive trajectories [12–17], which have also been investigated extensively in experiments [18–21].

In the standard quantum-jump method, named Monte Carlo wave function (MCWF), the state transformations induced by the jumps and their occurrence probabilities are directly fixed by the operators and coefficients of the master equation [3,10]. This allows one to associate each trajectory with a continuous selective measurement performed on the open system [22], so that the master equation can be seen as the result of the action of a non-selective observer, replacing the environment. However, the very definition of MCWF calls for a master equation with positive coefficients. Under some regularity conditions, this requirement is equivalent to the completely-positive(CP)-divisibility of the dynamics [23–25], meaning that the dynamics can be decomposed into intermediate completely positive maps. CP-divisibility has been introduced within the context of the definition of quantum Markovianity [26, 27] and its validity implies the absence of memory effects [23, 28, 29].

While generalizations of MCWF for master equations with negative coefficients have been introduced [30, 31], the possibility to extend the continuous-measurement picture beyond the realm of the CP-divisible evolutions has been extensively debated [32–

34]. Only very recently, a systematic approach has been put forward [35] to read the quantum-jump unraveling of non-CP-divisible evolutions in terms of continuous measurements. The approach relies on the definition of a proper rate operator [36–39] and it has hence been named rate operator quantum jumps (ROQJ). It is associated with a continuous-measurement scheme applying to any positive(P)-divisible dynamics [29,40–42], i.e., dynamics that can be decomposed into intermediate maps which are positive, but not necessarily completely positive. Such a scheme calls for an adjustment of the measurement apparatus conditioned on the previous sequence of outcomes, along the same lines of what happens in measurement-based feedback protocols [43–47].

In this paper, we define a class of jump unravelings interpolating between and combining the advantages of MCWF and ROQJ. We exploit the freedom in dividing any master equation into a deterministic and a jump part, possibly even mixing the contributions from the Hamiltonian and the dissipative terms. Besides its conceptual interest, this allows us to simplify the numerical and experimental implementation of the trajectories. On the one hand, we can select a fixed set of post-jump states for a well-defined class of master equations. On the other, we can instead set a desired time-independent, non-Hermitian linear operator ruling the deterministic evolution, also in the presence of an external time-dependent driving on the open system. Importantly, our analysis also shows that, under a constraint on P-divisible dynamics known as dissipativity [48], there exist (infinitely) many unravelings that can be associated with positive rate operators, bringing along different continuous-measurement schemes.

The rest of the paper is organized as follows. In Sec. 2, we present the notation and the general notions of quantum-jump unravellings that will be used throughout the paper, along with a detailed description of the continuous-measurement scheme associated with ROQJ unravelings. In Sec. 3, we introduce a whole class of rate-operator unravelings, which interpolates between MCWF and ROQJ and allows for a rather versatile control of the resulting trajectories. The positivity of such unravelings is discussed in Sec. 4, where we prove that it is guaranteed by dissipativity of the dynamics. Sec. 5 is devoted to an extended analysis of a case study, a two-level system dynamics where CP-divisibility is broken at any time, for which we compare the descriptions obtained via different ROQJ unravelings. Finally, the conclusions of our work are discussed in Sec. 6.

2 Quantum-jump unravelings

We start off by recalling briefly the formalism of quantum jumps to describe the dynamics of open quantum systems; in particular, we focus on the standard quantum-jump unraveling, i.e., MCWF [3,10], and the recently introduced ROQJ [35].

2.1 Open quantum system dynamics

We consider the evolution of finite-dimensional open quantum systems, given by the time-local master equation $d\rho(t)/(dt) = \mathcal{L}_t(\rho(t))$, where $\mathcal{L}_t$ is the generator

$$\mathcal{L}_t(\rho) = -i[H(t), \rho] + \mathcal{J}_t(\rho) - \frac{1}{2}\{\Gamma(t), \rho\}, \quad (1)$$

with $\mathcal{J}_t(\rho) = \sum_{\alpha=1}^{N^2-1} c_\alpha(t)L_\alpha(t)\rho L_\alpha^\dagger(t)$ and $\Gamma(t) = \sum_{\alpha=1}^{N^2-1} c_\alpha(t)L_\alpha^\dagger(t)L_\alpha(t)$, where N is the dimension of the open-system Hilbert space $\mathcal{H}_S$, $L_\alpha(t)$ and the Hamiltonian $H(t) = H^\dagger(t)$ are linear operators on $\mathcal{H}_S$, and $c_\alpha(t)$ are real functions of time. Importantly, $\mathcal{J}_t$ is a Hermiticity-preserving map and one has the duality relation

$$\Gamma(t) = \mathcal{J}_t^\dagger(\mathbb{1}), \quad (2)$$

where $\mathbb{1}$ is the identity operator and $\mathcal{J}_t^\dagger$ is the dual map of $\mathcal{J}_t$. The structure of the generator follows from the trace- and Hermiticity-preservation properties of the dynamics [49] $\Lambda_t = T\exp\left(\int_0^t d\tau \mathcal{L}_\tau\right)$ (T is the time-ordering operator); moreover, the functions $c_\alpha(t)$ can take negative values, yet with the resulting evolution being positive and even completely positive [1, 50]. On the other hand, under some regularity conditions [23–25], the positivity of the coefficients, $c_\alpha(t) \geq 0$ for every α and $t \geq 0$, is equivalent to the CP-divisibility of the dynamics, i.e, for any $t \geq s \geq 0$ one has the decomposition $\Lambda_t = V_{t,s}\Lambda_s$, where the so-called propagator $V_{t,s}$ is completely positive and trace preserving; CP-divisibility has been identified with quantum Markovianity in [26,27].

A crucial remark for our following analysis is that the representation of the generator $\mathcal{L}_t$ via Eq.(1) – with a Hamiltonian term, a Hermiticity-preserving map and an operator fixed by the duality relation (2) – is highly non-unique. In fact, one can define a new map

$$\mathcal{J}_t'(\rho) = \mathcal{J}_t(\rho) + \frac{1}{2}\left(\mathbf{C}(t)\rho + \rho\mathbf{C}^\dagger(t)\right), \quad (3)$$

with an arbitrary linear operator $\mathbf{C}(t)$ on $\mathcal{H}_S$, so that decomposing

$$\mathbf{C}(t) = A(t) + iB(t) \quad (4)$$

(with $A(t)$ and $B(t)$ Hermitian operators), together with

$$H'(t) = H(t) + \frac{1}{2}B(t), \quad \Gamma'(t) = \Gamma(t) + A(t), \quad (5)$$

the same generator $\mathcal{L}_t$ can be written as

$$\mathcal{L}_t(\rho) = -i[H'(t), \rho] + \mathcal{J}'_t(\rho) - \frac{1}{2}\{\Gamma'(t), \rho\} \quad (6)$$

and one still has

$$\Gamma'(t) = \mathcal{J}'^\dagger_t(\mathbb{1}); \quad (7)$$

indeed, $\Gamma'(t)$ is Hermiticity-preserving.

In the following we are going to introduce a class of jump unravelings where the map $\mathcal{J}'_t$ and the operator $\Gamma'(t)$ along with the Hamiltonian $H'(t)$ lead to, respectively, the jump and deterministic part of the trajectories; different unravellings of the same dynamics are thus defined for each set $\{H'(t), \mathcal{J}'_t, \Gamma'(t)\}$ such that the non-Hamiltonian terms satisfy the duality relation in Eq.(7) and that leads to the same generator $\mathcal{L}_t$. Let us stress that this is at variance with other jump unravelings, such as MCWF and ROQJ, which are instead typically defined starting from the Lindblad operators and coefficients ($L_\alpha(t)$ and $c_\alpha(t)$), and are thus not affected by the rewriting of the generator via Eq.(3)-(6).

2.2 Monte Carlo wave function vs rate operator quantum jumps

Both the MCWF and the ROQJ unravelings consist in piecewise deterministic processes on the set of pure states in $\mathcal{H}_S$, that is, they combine a deterministic time evolution and a jump process [1]. However, the specific form of the deterministic and jump parts are different in the two kinds of unraveling and, as a consequence, the range of applicability of the two methods is different.

In the case of CP-divisible dynamics, the master equation fixed by Eq.(1) can be unravelled by means of the MCWF method. The deterministic parts of the trajectories are fixed by the non-Hermitian linear operator

$$K(t) = H(t) - \frac{i}{2}\Gamma(t), \quad (8)$$

according to

$$|\psi(t)\rangle \rightarrow |\psi(t+dt)\rangle = \frac{(1 - iK(t)dt)|\psi(t)\rangle}{\|(1 - iK(t)dt)|\psi(t)\rangle\|}, \quad (9)$$

while the discontinuous parts, the jumps, are given by

$$|\psi(t)\rangle \rightarrow |\psi(t+dt)\rangle = \frac{L_\alpha(t)|\psi(t)\rangle}{\|L_\alpha(t)|\psi(t)\rangle\|}, \quad (10)$$

and each jump occurs between t and $t + dt$ with probability

$$p_{\psi(t),\alpha} = c_\alpha(t)\|L_\alpha(t)|\psi(t)\rangle\|^2 dt, \quad (11)$$

where dt is an infinitesimal time increment. It is clear that the previous formulation requires all the rates $c_\alpha(t)$ to be positive.

Extending the results of [36–38], recently in [35] it has been shown that such a requirement can be weakened considerably via the definition of a different quantum jump unraveling, named ROQJ. The latter relies on the definition of the rate operator

$$\mathbf{W}_\psi = \sum_{\alpha=1}^{N^2-1} c_\alpha(t)(L_\alpha(t) - \ell_{\psi,\alpha})P_\psi(L_\alpha(t) - \ell_{\psi,\alpha}(t))^\dagger, \quad (12)$$

with $\ell_{\psi,\alpha}(t) = \langle\psi|L_\alpha(t)|\psi\rangle$ and the projector $P_\psi = |\psi\rangle\langle\psi|$. As observed in [37, 38], $\mathbf{W}_\psi$ is directly associated with the time-local generator $\mathcal{L}_t$ and does not depend on its specific representation via $H(t), \mathcal{J}_t$ and $\Gamma(t)$: in fact, it can be equivalently written as

$$\mathbf{W}_\psi = (\mathbb{1} - P_\psi)\mathcal{L}_t(P_\psi)(\mathbb{1} - P_\psi). \quad (13)$$

The building block of ROQJ is the observation that $\mathbf{W}_\psi \geq 0$ for any state vector $|\psi\rangle$ if and only if the corresponding dynamics is P-divisible [51], i.e., for any $t \geq s \geq 0$ Λ_t can be decomposed as $\Lambda_t = V_{t,s}\Lambda_s$, and the propagator $V_{t,s}$ is trace preserving and positive, but not necessarily completely positive; P-divisibility, which is a significantly weaker requirement than CP-divisibility, has been identified with quantum Markovianity in [29, 42]. Focusing on P-divisible evolutions, one has then the spectral resolution

$$\mathbf{W}_{\psi(t)} = \sum_{k=1}^{N} \lambda_{\psi(t),k}|\varphi_{\psi(t),k}\rangle\langle\varphi_{\psi(t),k}|, \quad (14)$$

with $\lambda_{\psi(t),k} \geq 0$ for all k and $t \geq 0$. Introducing the non-Hermitian state-dependent operator

$$K_{\psi(t)} = K(t) + \Delta_{\psi(t)}, \quad (15)$$

with the non-linear correction

$$\Delta_{\psi(t)} = \frac{i}{2}\sum_{\alpha=1}^{N^2-1} c_\alpha(t)(2L_\alpha(t)\ell^*_{\psi,\alpha} - |\ell^*_{\psi,\alpha}|^2), $$

one realizes the jump unraveling as follows [35]: the deterministic evolution

$$|\psi(t)\rangle \rightarrow |\psi(t+dt)\rangle = \frac{(1 - iK_{\psi(t)}dt)|\psi(t)\rangle}{\|(1 - iK_{\psi(t)}dt)|\psi(t)\rangle\|} \quad (16)$$

is interrupted by the sudden jumps

$$|\psi(t)\rangle \rightarrow |\psi(t + dt)\rangle = \frac{V_{\psi(t),j}|\psi(t)\rangle}{\|V_{\psi(t),j}|\psi(t)\rangle\|}, \quad (17)$$

where

$$V_{\psi(t),j} = \sqrt{\lambda_{\psi(t),j}}|\varphi_{\psi(t),k}\rangle\langle\psi(t)|, \quad (18)$$

and the probability that the jump j occurs between t and $t + dt$ is

$$p'_{\psi(t),j} = \|V_{\psi(t),j}|\psi(t)\rangle\|^2 dt = \lambda_{\psi(t),j}dt; \quad (19)$$

indeed the deterministic evolution occurs with probability

$$p'^{det}_{\psi} = 1 - \sum_{j=1}^{N} p'_{\psi,j}. \quad (20)$$

Compared to MCWF, the operators $L_\alpha(t)$ and rates $c_\alpha(t)$ are replaced in ROQJ by the eigenvectors and eigenvalues of the rate operator $\mathbf{W}_{\psi(t)}$. This is the key that allows one to formulate a well-defined unraveling, with positive probabilities $p'_{\psi(t),j}$, for the set of P-divisible dynamics, rather than just for CP-divisible dynamics as in MCWF. For positive semigroups (for which the generator does not depend on time, $\mathcal{L}_t = \mathcal{L}$), a jump-unravelling fully equivalent to the ROQJ has been introduced in [37, 38], and further investigated (under the name of ortho-jumps) in [52, 53]; see also [54]. Later [35, 51], the positivity of the rate operator has been shown to be in one-to-one correspondence with the P-divisibility of the dynamics, thus extending the definition of the unraveling to this whole class of dynamics. In this paper, we show how it is possible to exploit the non-uniqueness of the master equation representation to define a whole class of positive unravelings.

Both MCWF and ROQJ can be extended to deal with, respectively, non-CP-divisible and non-P-divisible evolutions, via the use of reversed jumps connecting different trajectories [30, 31, 35]. However, ROQJ applies to general not necessarily P-divisible evolutions [35], and it can be used to treat certain non-CP-divisible dynamics [55–57] where the non-Markovian version of MCWF cannot be used.

Finally, we stress that the ROQJ involves the diagonalization of the rate operator, which adds complexity to the actual implementation of the unraveling. On the other hand, such a diagonalization concerns an $N \times N$ matrix and it is thus significantly simpler, for example, than the direct diagonalization of the $N^2 \times N^2$ matrix associated with the generator of the master equation. In addition, crucially, the diagonalization in ROQJ needs not to be done at each time step, contrary to what would happen for example

in a diffusive unraveling [51]. Rather, one has to diagonalize the rate operator only if a jump occurs and jumps are indeed rare events, whose probability is proportional to the infinitesimal time step dt. The key point is that one can fix whether a jump occurs or not by looking at the deterministic part of the evolution only, as the probability of having any jump is

$$\sum_j p'_{\psi(t),j} = \sum_j \lambda_{\psi(t),j}dt = \text{Tr}\left\{\mathbf{W}_{\psi(t)}\right\}dt, \quad (21)$$

where Tr denotes the trace, which leads us to (neglecting as usual terms of order dt^2)

$$\sum_j p'_{\psi(t),j} = 1 - \|(1 - iK(t)dt)|\psi(t)\rangle\|^2. \quad (22)$$

Therefore, since we know the operator $K(t)$ giving the deterministic evolution, we need to construct the rate operator and diagonalize it only at those (rare) times when a jump takes place. Note that an analogous reasoning applies to the rate operators $\mathbf{R}_\psi$ described in the following.

2.3 Continuous-measurement scheme

Both in MCWF [22] and in ROQJ [35] unraveling the trajectories can be seen as due to a continuous measurement on the open system. The state transformations and corresponding probabilities can be associated with a quantum instrument [58], mapping the set of outcomes into a set of open-system completely positive trace non-increasing maps that sum up to a trace preserving map, but, crucially, in ROQJ continuous-measurement schemes can be defined for the whole set of P-divisible dynamics.

Let us in fact consider the rate operator $\mathbf{W}_\psi$ of a P-divisible dynamics, and the corresponding jump operators $\{V_{\psi,j}\}_{j=1,...N}$ and jump probabilities $\{p'_{\psi,j}\}_{j=1,...N}$ defined as in Eqs.(18) and (19). In addition, let us denote as $V_{\psi,\emptyset}$ the operator obtained from the first-order evolution associated with the effective Hamiltonian in Eq.(15) according to

$$V_{\psi,\emptyset} = (1 - iK_\psi dt)|\psi\rangle\langle\psi|, \quad (23)$$

and as $p'_{\psi,\emptyset} = p'^{det}_\psi$ the probability of having a deterministic evolution according to Eq.(20). It is then readily seen that these operators and probabilities correspond to the state transformations and associated probabilities of a well-defined quantum instrument, for any fixed $|\psi\rangle \in \mathcal{H}_S$.

Take in fact the set of outcomes $\mathcal{O} = \{a, \emptyset, j\}_{j=1,...N}$ and the maps $\{\mathcal{I}_{\psi,j}\}_{j=a,\emptyset,1,...N}$ whose action on a generic state ρ on $\mathcal{H}_S$ is given by

$$\mathcal{I}_{\psi,j}(\rho) = V_{\psi,j}\rho V^\dagger_{\psi,j} \quad j = a, \emptyset, 1, \ldots N, \quad (24)$$

where we introduced also the (auxiliary) outcome a, along with the operator $V_{\psi,a} = \mathbb{1} - |\psi\rangle\langle\psi|$. Now, for any fixed $|\psi\rangle \in \mathcal{H}_S$, the maps in Eq.(24) are indeed completely positive and trace non-increasing and they sum up to a trace preserving map, since $\sum_{j=a,\emptyset,1,\dots N} V_{\psi,j}^{\dagger} V_{\psi,j} = \mathbb{1}$, as follows from Eqs.(14), (18), (21) and (22). Thus, the state transformations and associated probabilities

$$\rho \mapsto \frac{\mathcal{I}_{\psi,j}(\rho)}{\mathrm{Tr}\left\{\mathcal{I}_{\psi,j}(\rho)\right\}} \qquad \mathcal{P}_{\psi,j} = \mathrm{Tr}\left\{\mathcal{I}_{\psi,j}(\rho)\right\} \qquad (25)$$

correspond to the post-measurement states and probabilities of the measurement with outcomes $\mathcal{O}$ and described by the quantum instrument $\{\mathcal{I}_{\psi,j}\}_{j=a,\emptyset,1,\dots N}$. But if we now focus on the action of the maps on the pure state $\rho = |\psi\rangle\langle\psi|$, we see that the state transformations and probabilities in Eq.(25) for $j = 1,\dots,N$ are nothing else than, respectively, the state after the jump as in Eqs.(18) and the jump probability in (19), $\mathcal{P}_{\psi,j} = p'_{\psi,j}$, while for $j = \emptyset$ we get the deterministic evolution in Eq.(16) and the probability in Eq.(20), $\mathcal{P}_{\psi,\emptyset} = p'_{\psi,\emptyset}$, where the latter follows from the identity in Eq.(22); on the other hand, the (auxiliary) outcome a occurs with zero probability, $\mathcal{P}_{\psi,a} = 0$. The instrument in Eq.(24) can be realized, for example, by N counters surrounding the system and parametrized by the index j: a click of the j-th counter indicates that the system jumps to the j-th eigenstate of $\mathbf{W}_\psi$. Importantly, also the scenario where no counter clicks corresponds to a measurement performed on the system, with null result $\emptyset$ [59] and, as said, resulting in the evolution fixed by Eq.(23).

If we now consider any trajectory of the jump unraveling[1] defined by $\mathbf{W}_\psi$ in Sec.2.2, we can repeat the reasoning above for any infinitesimal time dt starting from any pure initial state $|\psi_0\rangle$, which means that such a trajectory is equivalently obtained as the result of a continuous measurement performed on the quantum system associated with $\mathcal{H}_S$ and described by the quantum instrument in Eq.(24). As a consequence, the open-system dynamics fixed by the master equation (1) and resulting from the average over the trajectories of the unraveling is equivalently obtained as the consequence of a continuous non-selective monitoring of the system at hand, meaning that one is continuously measuring the system via the measurement apparatus described by the instrument in Eq.(24), but without selecting the system according to the measurement outcomes.

---

[1]On more precise mathematical terms, one should consider a stochastic pure state, that is a stochastic process with values in $\mathcal{H}_S$, defined by a counting process whose trajectories correspond to the sequences of jumps [22,35].

Crucially, the instrument to be applied on each trajectory at any time t depends on the (stochastic) state $|\psi(t)\rangle$ or, equivalently, on the previous sequence of events, which is what allows us to introduce a proper continuous-measurement scheme in the presence of P-divisible, but not necessarily CP-divisible dynamics [35]. On a practical level, this means that the actual realization of the continuous-measurement scheme described in this section calls for a continuous adjustment of the measurement apparatus monitoring the system, depending on the sequence of outcomes. While the strategy to implement this procedure will crucially depend on the specific experimental platform at hand, we can already point to a correspondence with the adaptive approaches that characterize, for example, the measurement-based feedback strategies described in [45–47], where the measurement basis is changed dynamically and according to the previous sequence of measurement outcomes.

3 A new class of rate operator quantum jumps

We are now ready to present a novel class of quantum-jump unravelings, which is based on a family of rate operators defined starting from Eqs.(3)-(5). This class combines features of both MCWF, allowing for a linear effective Hamiltonian, and the ROQJ discussed above, being positive for dynamics with possibly negative rates. In addition, we show how the freedom in choosing the rate operator allows us to control and manipulate some basic properties of the trajectories of the unraveling, which can be useful for the numerical simulation of the dynamics and the actual experimental implementation of the jumps.

3.1 Definition of the unravelings

The basic observation to define the class of ROQJs is that $\mathbf{W}_\psi$ in Eq.(13) can also be written as

$$\mathbf{W}_\psi = (\mathbb{1} - P_\psi)\mathbf{R}_\psi(\mathbb{1} - P_\psi), \qquad (26)$$

where

$$\mathbf{R}_{\psi(t)} = \mathcal{J}_t(|\psi(t)\rangle\langle\psi(t)|). \qquad (27)$$

Now, if $\mathbf{R}_{\psi(t)} \geq 0$ for any $|\psi(t)\rangle$ one can define a jump unraveling that merges (8)-(9) with (17)-(18); that is, the deterministic evolution is governed by (9), but the jumps are realized via

$$|\psi(t)\rangle \to |\psi(t+dt)\rangle = \frac{R_{\psi(t),k}|\psi(t)\rangle}{\|R_{\psi(t),k}|\psi(t)\rangle\|}, \qquad (28)$$

with

$$R_{\psi(t),k} = \sqrt{r_{\psi(t),k}}|\phi_{\psi(t),k}\rangle\langle\psi(t)|, \qquad (29)$$

and the probability that the jump k occurs between t and $t + dt$ reads now

$$p''_{\psi(t),k} = \|R_{\psi(t),k}|\psi(t)\rangle\|^2 dt = r_{\psi(t),k}\, dt; \qquad (30)$$

indeed, $r_{\psi(t),k}$ and $|\phi_{\psi(t),k}\rangle$ are the eigenvalues and eigenvectors of $\mathbf{R}_{\psi(t)}$, i.e.,

$$\mathbf{R}_{\psi(t)} = \sum_{k=1}^{N} r_{\psi(t),k}|\phi_{\psi(t),k}\rangle\langle\phi_{\psi(t),k}| \qquad (31)$$

and the deterministic evolution will occur with probability $p''^{det}_{\psi(t)} = 1 - \sum_{k=1}^{N} p''_{\psi(t),k}$. General conditions guaranteeing the positivity of $\mathbf{R}_{\psi(t)}$ will be presented in Sec. 4. We stress that whenever $\mathbf{R}_{\psi(t)}$ is positive the analysis performed in Sec.2.3 can be readily adapted to the unraveling fixed by this rate operator, so that a continuous-measurement scheme can be defined via a quantum instrument with maps $\mathcal{I}_{\psi,j}$ as in Eq.(24), where $\{V_{\psi,j}\}_{j=1,\ldots N}$ are indeed replaced by $\{R_{\psi,k}\}_{k=1,\ldots N}$, while the operator $V_{\emptyset,j}$ corresponding to the outcome $\emptyset$ and associated with the deterministic evolution is now fixed by the effective Hamiltonian in Eq.(8), compare with Eq.(23).

Before proving that the construction fixed by Eqs.(27)-(31) provides us with a well-defined unraveling of the master equation (1) whenever the rate operator is positive, let us stress that it avoids the non-linear correction in the non-Hermitian operator fixing the deterministic evolution, still potentially allowing for positive probabilities in the case of non-CP-divisible evolutions; $p''_{\psi(t),k} \geq 0$ is in fact equivalent to the requirement that the map $\mathcal{J}_t$ is positive for all $t \geq 0$, which is significantly weaker than CP-divisibility as we will see in Sec. 4. Moreover, the definition of the rate operator $\mathbf{R}_{\psi(t)}$ in Eq.(27) does depend on the specific choice of the map $\mathcal{J}_t$ in the representation of the generator $\mathcal{L}_t$ as in Eq.(1); as a consequence, Eqs.(9), (28) and (30) define a whole family of unravelings, corresponding to different choices of the operator $\mathbf{C}(t)$ in Eqs.(3)-(5). We denote these unravelings with $\mathbf{R}$-ROQJ, specifying the explicit form of the rate operator $\mathbf{R}$ when needed; furthermore, we will refer to the ROQJ unraveling discussed in Sec. 2.2 as $\mathbf{W}$-ROQJ.

Proof. Given the pure state $|\psi(t)\rangle\langle\psi(t)|$ at time t, the deterministic evolution will occur with probability

$$p''^{det}_{\psi(t)} = 1 - \sum_{k=1}^{N} p''_{\psi(t),k} = 1 - \mathrm{Tr}\left\{\mathbf{R}_{\psi(t)}\right\} dt, \qquad (32)$$

where in the last equality we used Eq.(31). But using Eq.(27) along with

$$\Gamma(t) = \mathcal{J}_t^\dagger(\mathbb{1}), \qquad (33)$$

we get

$$\begin{aligned} p''^{det}_{\psi(t)} &= 1 - \mathrm{Tr}\left\{\mathcal{J}_t(|\psi(t)\rangle\langle\psi(t)|)\right\} dt \\ &= 1 - \langle\psi(t)|\Gamma(t)|\psi(t)\rangle dt, \qquad (34) \end{aligned}$$

which highlights the role of the duality relation in Eq.(33) to express the probability of the deterministic evolution in terms of both the jump part of the master equation $\mathcal{J}_t$ and the term $\Gamma(t)$ entering into the non-Hermitian operator in Eq.(8). The deterministic evolution will map the pure state $|\psi(t)\rangle\langle\psi(t)|$ into the pure state (see Eq.(9))

$$\begin{aligned} &\frac{(1 - iK(t)dt)|\psi(t)\rangle\langle\psi(t)|(1 + iK^\dagger(t)dt)}{\|(1 - iK(t)dt)|\psi(t)\rangle\|^2} \\ &= \frac{(1 - iK(t)dt)|\psi(t)\rangle\langle\psi(t)|(1 + iK^\dagger(t)dt)}{p''^{det}_{\psi(t)}}, \qquad (35) \end{aligned}$$

where we used Eqs.(8) and (34) in the denominator (neglecting the terms of order dt^2).

On the other hand, as said, given the state $|\psi(t)\rangle\langle\psi(t)|$ at time t, we will have the jump described by $R_{\psi(t),k}$ in Eq.(29), i.e. (compare with Eq.(28))

$$|\psi(t)\rangle\langle\psi(t)| \to \frac{R_{\psi,k}|\psi(t)\rangle\langle\psi(t)|R_{\psi,k}^\dagger}{\|R_{\psi,k}|\psi(t)\rangle\|^2} = |\phi_{\psi(t),k}\rangle\langle\phi_{\psi(t),k}|, \tag{36}$$

with probability as in Eq.(30).

All in all, if we average the state at time $t + dt$ over the trajectories where the state at time t is $|\psi(t)\rangle\langle\psi(t)|$, we get the mixture of the states obtained via the deterministic evolution or one of the jumps, each weighted with the corresponding probability: using Eqs.(35), (36) and (30), such a (conditioned) average corresponds to

$$\begin{aligned} &p''^{det}_{\psi(t)}\frac{(1 - iK(t)dt)|\psi(t)\rangle\langle\psi(t)|(1 + iK^\dagger(t)dt)}{p''^{det}_{\psi(t)}} \\ &+ \sum_{k=1}^{N} r_{\psi(t),k}|\phi_{\psi(t),k}\rangle\langle\phi_{\psi(t),k}|\, dt \\ &= |\psi(t)\rangle\langle\psi(t)| - i\left[H, |\psi(t)\rangle\langle\psi(t)|\right] dt \\ &- \frac{1}{2}\{\Gamma(t), |\psi(t)\rangle\langle\psi(t)|\} dt + \mathcal{J}_t(|\psi(t)\rangle\langle\psi(t)|)dt, \tag{37} \end{aligned}$$

where the equality is due to Eqs.(8), (27) and (31), and we neglected the terms of order dt^2. Finally, we perform a second average, this time with respect to the pure states $|\psi(t)\rangle\langle\psi(t)|$ we fixed at time t, so that we get the average over all the trajectories; the previous expression then yields the first order expansion of the time-local master equation $d\rho(t)/(dt) = \mathcal{L}_t(\rho(t))$ with $\mathcal{L}_t$ as in Eq.(1), which concludes the proof. $\square$

Indeed, the proof above does not depend on the specific representation of the generator $\mathcal{L}_t$ and then it holds for any choice of the operator $\mathbf{C}$, as long as the corresponding rate operator $\mathbf{R}_{\psi(t)}$ is positive. Going beyond the results in [35], we have thus defined a new class of unravelings of the master equation (1) for P-divisible dynamics, which are equipped with an associated continuous-measurement scheme, see the discussion after Eq.(31). Besides including the simpler linear effective Hamiltonian that characterizes the MCWF method and connecting the positivity of the rate operator with a significant property of the dynamics, as proved in Sec.4, the use of distinct master-equation representations allows us to control the deterministic and jump parts of the unraveling in a versatile way, as we are now going to show.

3.2 R-ROQJ with fixed post-jump states

First of all, a proper choice of $\mathbf{C}$ can be used to simplify to a significant extent the jumps in the unraveling. An explicit condition for this can be derived for two-dimensional open quantum systems, i.e., $\mathcal{H}_S = \mathbb{C}^2$.

Given any time-local generator $\mathcal{L}_t$ on the set of linear operators $\mathcal{B}(\mathbb{C}^2)$ in the GKLS form as in Eq.(1), $\mathcal{J}_t$ can be represented via the 16 parameters $J_{ij}^{kl}(t)$ defined by

$$J_{ij}^{kl}(t) = \langle i | \, \mathcal{J}_t[|k\rangle \langle l|] \, |j\rangle \quad i,j = 1,2, \qquad (38)$$

with respect to any orthonormal basis $\{|1\rangle, |2\rangle\}$; note that the Hermiticity-preservation condition implies $\left(J_{ij}^{kl}(t)\right)^* = J_{ji}^{lk}(t)$. Now, if there is a basis such that

$$J_{ij}^{kl}(t) = (J_{ij}^{kl}(t))^* \quad \forall i,j,k,l = 1,2, \qquad (39)$$

i.e., the Choi matrix associated with $\mathcal{J}_t$ is real, and the deterministic evolution in-between the jumps does not introduce a relative phase when acting on the basis elements, it is possible to define a rate operator $\mathbf{R}_{\psi(t)}$ via Eqs.(3) and (27) whose eigenvectors are independent from the pre-jump state $|\psi(t)\rangle$. This implies that the post-jump states are always the same, so that the trajectories are fixed by at most 3 deterministically-evolving states, which results in a strong simplification of both the numerical simulation and the experimental implementation of the corresponding unraveling, as will also be shown by means of an example in Sec.5. More explicitly, we have in fact the following.

Proposition 1. *Given the master equation (1) for $N = 2$, if there is an orthonormal basis of $\mathbb{C}^2$, denoted as $\{|\varphi_1\rangle, |\varphi_2\rangle\}$, and a time-dependent linear operator $\mathbf{C}(t) \in \mathcal{B}(\mathbb{C}^2)$ with matrix representation in this basis*

$$\mathbf{C}(t) = \qquad (40)$$
$$\begin{pmatrix} J_{22}^{11}(t) - J_{11}^{11}(t) + ix(t) & y(t) \\ y(t) + 2(J_{11}^{12}(t) - J_{22}^{12}(t)) & J_{11}^{22}(t) - J_{22}^{22}(t) + ix(t) \end{pmatrix}$$

with $x(t), y(t)$ two real functions, such that

- *the jump operator $\mathcal{J}_t'$ fixed by Eq.(3) satisfies Eq.(39);*

- *if the state $|\psi(t)\rangle$ at time t is in the form*

$$|\psi(t)\rangle = c(t) |\varphi_1\rangle \pm \sqrt{1 - c(t)^2} |\varphi_2\rangle \qquad (41)$$

  for some $-1 \leq c(t) \leq 1$, the deterministic evolution fixed by Eqs.(5), (8) (with H' instead of H and Γ' instead of Γ) and (9) implies that the state at time $t + dt$ is in the form

$$|\psi(t + dt)\rangle = a(t,dt) |\varphi_1\rangle \pm \sqrt{1 - a(t,dt)^2} |\varphi_2\rangle \qquad (42)$$

  for some $-1 \leq a(t,dt) \leq 1$;

- *the rate operator $\mathbf{R}_{\psi(t)} = \mathcal{J}_t'(|\psi(t)\rangle\langle\psi(t)|)$ is positive for any state $|\psi(t)\rangle$ as in Eq.(41);*

and we restrict to

- *initial states $|\psi_0\rangle = |\psi(0)\rangle$ in the form as in Eq.(41),*

then there exists a jump unraveling that involves only the 3 families of states $\{|\psi_0(t)\rangle, |\varphi_+(t,s)\rangle, |\varphi_-(t,s)\rangle\}$, which are deterministically evolved from $\left\{|\psi_0\rangle, |\varphi_\pm\rangle = \frac{1}{\sqrt{2}}(|\varphi_1\rangle \pm |\varphi_2\rangle)\right\}$ via

$$D(t,s) = T \exp\left(-i \int_s^t d\tau \left(H'(\tau) - \frac{i}{2}\Gamma'(\tau)\right)\right). \qquad (43)$$

The conditions in Eqs.(41) and (42) mean that the unraveling will involve exclusively pure states without a relative phase in the basis $\{|\varphi_1\rangle, |\varphi_2\rangle\}$, if this is the case at the initial time; this is also why the positivity requirement on the rate operator $\mathbf{R}_{\psi(t)}$ can be now restricted only to states of this form. In practice, the deterministic evolution between two times s and t will be given by the operator in Eq.(43), which indeed corresponds to the effective non-Hermitian Hamiltonian fixed by Eq.(5) for the operator $\mathbf{C}(t)$ as in Eq.(40). The jumps at time t, given by the eigenvectors of $\mathbf{R}_{\psi(t)}$, will always end up in one of the eigenvectors $\{|\varphi_+\rangle, |\varphi_-\rangle\}$, and then all in all the trajectories will consist of piecewise deterministic evolutions among $\{|\psi_0(t)\rangle, |\varphi_+(t,s)\rangle, |\varphi_-(t,s)\rangle\}$. Note that the probabilities of having the jumps between time t and $t + dt$ are fixed by the eigenvalues of $\mathbf{R}_{\psi(t)}$, so that different matrices $\mathbf{C}(t)$ in Eq.(40) will generally define distinct unravelings, with the same trajectories but different associated probabilities.

In addition, the existence of a class of ROQJ can be exploited to control to a large extent the deterministic

evolution in-between the jumps. From Eqs.(4), (5) and (8) we see how any effective non-Hermitian Hamiltonian can be enforced by means of a proper choice of $\mathbf{C}$, which will also result in a modified set of jump states and probabilities, according to Eq.(3), (27) and (30). As will be shown by means of a significant example in Sec.5, this choice can be made while keeping the positivity of the rate operator and it is particularly convenient for driven systems. We stress that the definition of different partitions between the deterministic and the jump parts of the unraveling, starting from distinct representations of the same master equation (1) by virtue of Eqs.(3)-(6), is not encompassed by the possibility to define different unravelings that is routinely used in MCWF, which relies on the invariance of the generator under unitary transformations of the set of Lindblad operators [1] and would not affect the partition of the generator as dictated by Eq.(6) and (7); compare with the remark at the end of Sec.2.1.

4 Positivity of the rate operators

We can now complete the definition of the $\mathbf{R}$-ROQJ by deriving general conditions ensuring that it is associated with a positive rate operator. Besides justifying the construction in Eqs.(28) and (30), this also guarantees the existence of a fully consistent continuous-measurement picture as discussed in Sec.2.3.

Clearly, if the evolution is CP-divisible, not only both MCWF and $\mathbf{W}$-ROQJ are well defined, but one can always find a completely positive map $\mathcal{J}_t$ giving rise to a positive $\mathbf{R}$-ROQJ. Instead, any P-divisible evolution does guarantee positivity of $\mathbf{W}_{\psi(t)}$, but not necessarily the positivity of $\mathbf{R}_{\psi(t)}$. Still, we note that P-divisibility constrains the number of possible negative eigenvalues of the rate operator $\mathbf{R}_{\psi(t)}$. We have in fact the following:

Proposition 2. *For any P-divisible evolution, $\mathbf{R}_{\psi(t)}$ can have at most one negative eigenvalue.*

Proof. The proof easily follows from the min-max principle for Hermitian matrices: let A be a Hermitian $n \times n$ matrix, and let

$$\lambda_n \geq \lambda_{n-1} \geq \ldots \geq \lambda_1$$

be the real eigenvalues of A. Then

$$\lambda_k = \max_{\Sigma} \min_{x \in \Sigma} \langle x | A | x \rangle \qquad (44)$$

where x is normalized, and Σ is a $(n-k+1)$-dimensional subspace of $\mathbb{C}^n$.

Now, since $\mathbf{W}_\psi = (\mathbb{1} - P)\mathbf{R}_\psi(\mathbb{1} - P) \geq 0$, one has for any $x \in \Sigma = (\mathbb{1} - P)\mathbb{C}^n$

$$\langle x | \mathbf{R}_\psi | x \rangle = \langle x | \mathbf{W}_\psi | x \rangle \geq 0.$$

Hence, from (44) one finds $\lambda_2 \geq 0$ (since in (44) one maximizes over all Σs), and hence only λ_1 may be negative. $\qquad \square$

We stress that the proof does not depend on the specific $\mathcal{J}_t$ used to represent the generator $\mathcal{L}_t$ and hence applies to any $\mathbf{R}$-ROQJ.

Now, since $\mathbf{R}_{\psi(t)}$ does depend upon the specific $\mathcal{J}_t$, see Eq.(27), a natural strategy to ensure the positivity of $\mathbf{R}_{\psi(t)}$ arises: is it possible to use the freedom introduced by (3) so that the rate operator defined in terms of $\mathcal{J}'_t$ is positive? Interestingly, in all the examples we analyzed this is the case; however, we can give a positive answer in generality only for a class of P-divisible evolutions that enjoys an additional property. In the Heisenberg picture P-divisibility means that the propagators $V_{t,s}^\dagger$ are positive and unital. It is well known [60, 61] that this implies the Kadison-Schwarz inequality

$$V_{t,s}^\dagger(X^\dagger X) \geq V_{t,s}^\dagger(X^\dagger)V_{t,s}^\dagger(X), \qquad (45)$$

for all Hermitian operators $X = X^\dagger \in \mathcal{B}(\mathcal{H}_S)$. A more restricted class of evolutions is thus defined by propagators that satisfy (45) for all X, not necessarily Hermitian. This leads us to the identification of the condition ensuring the positivity of the $\mathbf{R}$-ROQJ:

Proposition 3. *If the propagators of the dynamics satisfy (45) for all $X \in \mathcal{B}(\mathcal{H}_S)$, there exists a representation of the master equation (1) with a positive map $\mathcal{J}_t$, which we denote as $\mathbf{J}_t$.*

The proof, which is reported in Appendix B, is based on some techniques introduced by Lindblad in his seminal paper [48], based on the fact that the Kadison-Schwarz inequality may be rephrased by the following condition for the time-local generator (in the Heisenberg picture):

$$\mathcal{L}_t^\dagger(X^\dagger X) \geq \mathcal{L}_t^\dagger(X^\dagger)X + X^\dagger \mathcal{L}_t^\dagger(X), \qquad (46)$$

again for all $X \in \mathcal{B}(\mathcal{H}_S)$ and $t \geq 0$. The generators satisfying Eq.(46) are called dissipative [48]. All in all, the dissipativity condition is equivalent to P-divisibility if one restricts to Hermitian operators X; however, assuming that the condition (46) holds for all $X \in \mathcal{B}(\mathcal{H}_S)$ the corresponding evolution is not only P-divisible but in addition the propagator $V_{t,s}$ satisfies (45).

From the physical point of view, the dissipativity condition can be understood with the following remark: let $\varrho(t)$ be an instantaneous invariant state, i.e. $\mathcal{L}_t(\varrho(t)) = 0$. One has $\text{Tr}(\varrho(t)\mathcal{L}_t^\dagger(X^\dagger X)) = \text{Tr}(\mathcal{L}_t(\varrho(t))(X^\dagger X)) = 0$, and hence introducing the

following inner product in the space of Hermitian operators

$$(X, Y)_\varrho = \text{Tr}(\varrho X^\dagger Y)$$

the formula (46) implies [25]

$$\text{Re}\,(X, \mathcal{L}_t^\dagger(X))_{\varrho(t)} \leq 0, \qquad (47)$$

for any operator $X \in \mathcal{B}(\mathcal{H}_S)$. In particular, if $|i(t)\rangle$ defines an eigenbasis of $\varrho(t)$, then taking $X = |i(t)\rangle\langle j(t)|$ the condition (47) clearly shows that P-divisibility provides constraints for populations ($i = j$), whereas dissipativity is more restrictive, providing constraints also for coherences ($i \neq j$).

Summarizing, the condition in Eq.(45), or equivalently Eq.(46), for all $X \in \mathcal{B}(\mathcal{H}_S)$ allows for a representation of (1) with a positive map $\mathbf{J}_t$. In other terms, dissipativity guarantees the existence of a rate operator $\mathbf{R}_{\psi(t)}$, defined from $\mathbf{J}_t$ by Eq.(27), such that the unraveling given by Eqs.(9), (28) and (30) is well-defined, as $\mathbf{R}_{\psi(t)} \geq 0$ for any $\psi(t)$. As follows from the discussion in Sec.2.3 and 3.1, this also means that dissipativity ensures the possibility to obtain the dynamics as the result of a continuous non-selective measurement on the system at hand. It should be stressed that the representation with a positive map $\mathbf{J}_t$ is not unique, corresponding to a non-unique continuous-measurement scheme, as we will see explicitly in the examples in the next section. The use of the $\mathbf{R}$-ROQJ allows thus for a versatile definition of the deterministic and jump parts of the unraveling that, along with the dissipativity of the dynamics, result in distinct experimental procedures leading to the detection of trajectories associated with different unraveling of the same master equation.

5 Eternally non-Markovian qubit master equation

To explore in an explicit case study the different possible $\mathbf{R}$-ROQJ unravelings and compare them among each other, as well as with the $\mathbf{W}$-ROQJ, we consider the two-level system dynamics fixed by the following generator

$$\mathcal{L}_t(\rho) = i\frac{b(t)}{2}[\sigma_z, \rho] + \frac{1}{2}\sum_{k=1}^{3}\gamma_k(t)(\sigma_k\rho\sigma_k - \rho), \quad (48)$$

where σ_k are the Pauli spin operators. Such a master equation has been studied extensively in the literature [55–57], since, despite its simplicity, it possesses several interesting features. The open-system evolution fixed by Eq.(48) can arise as due to an average over randomly distributed unitary evolutions [56] or as the classical

mixture of Markovian dephasing dynamics in three different directions [57]. In particular, for some choices of the rates $\gamma_k(t)$ the resulting dynamics is P-divisible, while CP-divisibility is broken for any $t > 0$. This kind of dynamics is usually referred to as eternally non-Markovian, indicating that the backflow of information to the open system witnessed by the negativity of the decay rate continues for the whole evolution; hence, any Markovian limit, even in the asymptotic time scale, is precluded. Most importantly for our purpose, eternally non-Markovian dynamics cannot be treated by means of the MCWF at any time of the evolution. Even more, also a powerful non-Markovian generalization of MCWF, named non-Markovian quantum jumps [30,31], cannot be applied in this case since CP-divisibility is violated from the very beginning of the dynamics. The general ingredients for the implementation of the jump methods, including the relevant numerical aspects, can be found from references [10,11,62].

It is important to stress that the smaller the effective ensemble size N_{eff} the more efficiently the simulations can be implemented and optimized. This is because it is enough to generate N_{eff} state vector evolutions and decide N times at each time step whether the jump happened or not; here, N is the size of the total ensemble. This allows us to track how many members of the total ensemble are in each of the N_{eff} different members of the effective ensemble, avoiding repetitions of identical evolutions in a given interval of time. As we are going to show explicitly for the dynamics at hand, we can control N_{eff} by choosing different ROs, which opens considerable prospects for an efficient implementation of the simulations also when dealing with more complicated dynamics.

5.1 Undriven master equation

We set at first $b(t) = 0$ and study the case where we have a P-divisible evolution even if one of the rates is temporally negative, i.e., CP-divisibility is broken; we suppose in particular that $\gamma_3(t) < 0$ for any $t > 0$. Then Λ_t is P-divisible provided that $\gamma_1(t), \gamma_2(t) \geq |\gamma_3(t)|$. Dissipativity requires the stronger condition [63] that $\gamma_1(t), \gamma_2(t) \geq 2|\gamma_3(t)|$. Interestingly, it turns out that whenever $\gamma_3(t) < 0$ the map $\mathcal{J}_t(\rho) = \sum_{k=1}^{3} \gamma_k(t)\sigma_k\rho\sigma_k/2$ is not positive. However, if the generator (48) gives rise to a P-divisible evolution, one can define different positive $\mathbf{R}$-ROQJ by means of different operators $\mathbf{C}(t)$ in Eqs.(3)-(5).

Unraveling with $\mathbf{R1}$

The first choice we make is to use
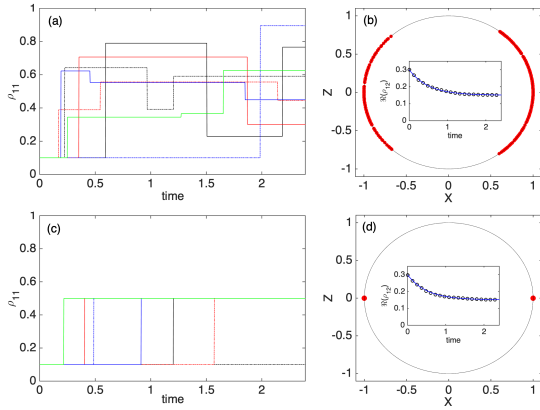
$$\mathbf{C}(t) = \frac{\gamma(t)}{2}\mathbb{1} \qquad (49)$$

Figure 1: Simulation results using rate operator **R1** [(a), (b)] and **R2** [(c), (d)] for model (48) without driving. Example trajectories are displayed in (a) and (c). Final steady state distributions for Bloch vector X and Z components are shown in (b) and (d). The insets in (b) and (d) demonstrate the agreement between the analytical results (solid line) and simulation results (dots) with 10^4 trajectories. The error bars are similar to the size of the dots.

with

$$\gamma(t) = \sum_k \gamma_k(t),$$

as the corresponding map

$$\mathbf{J}_t(\rho) = \mathcal{J}_t(\rho) + \frac{\gamma(t)}{2}\rho \qquad (50)$$

is positive, as shown in Appendix C. In particular for the eternally non-Markovian evolution [55, 57] defined by $\gamma_1 = \gamma_2 = 1$, and $\gamma_3(t) = -\tanh t$, one has a P-divisible evolution, but the corresponding generator $\mathcal{L}_t^\dagger = \mathcal{L}_t$ is not dissipative. Nevertheless, the map $\mathbf{J}_t$ is positive and one can define the positive rate operator $\mathbf{R1}_{\psi(t)} = \mathbf{J}_t(|\psi(t)\rangle\langle\psi(t)|) \geq 0$. The deterministic evolution is fixed by $K1(t) = \frac{i}{2}\gamma(t)\mathbb{1}$. Figure 1 (a) shows 7 example pure-state trajectories, with initial state $|\psi(0)\rangle = \sqrt{0.1}|1\rangle + \sqrt{0.9}|2\rangle$, and the probability ρ_{11} of the state $|1\rangle$. Figure 1 (b) displays the final distribution of the Bloch vector X and Z components over the trajectories while the inset shows the agreement between the analytical results and simulations for the coherence ρ_{12}.

Unraveling with **R2**

The second choice we make takes advantage of the general result for qubits dynamics in Proposition 1. In fact, as we show explicitly in Appendix D, the eternal non-Markovian evolution satisfies the assumptions of the mentioned proposition, meaning that it is possible to define a **R**-ROQJ with a fixed set of (deterministically evolving) states after

the jumps. Actually, in Appendix D we define a continuous family of rate operators with fixed post-jump states for the eternal non-Markovian dynamics, also ensuring their positivity. Quite interestingly, this means that there exists a continuous family of continuous measurement schemes for the same open-system dynamics originating from the non-unique decomposition (6) of the generator. We stress that this freedom is inherently different from the well-known [1] unitary freedom in defining the operators that appear in the master equation (1). Moreover, the instruments defining the different measurement schemes, as well as the associated probabilities, will generally be different, while the post-measurement states will be the same.

A special instance of the **R**-ROQJs with fixed post-jump states is given by

$$\mathbf{R2}_{\psi(t)} = \mathbf{R1}_{\psi(t)} - \gamma_3(t)|\psi(t)\rangle\langle\psi(t)| \qquad (51)$$

associated with the deterministic evolution $K2(t) = \frac{i}{2}[\gamma_1(t) + \gamma_2(t)]\mathbb{1}$. The corresponding simulation results are shown in Fig. 1 (c) and (d). The example trajectories in Fig. 1 (c) illustrate that the ensemble consists now a discrete set of pure states. In the final distribution of states, see Fig. 1 (d), we have only two states $|\pm\rangle = \frac{1}{\sqrt{2}}(|1\rangle \pm |2\rangle)$. As a matter of fact, during the whole simulation, only three states appear: the initial state and $|\pm\rangle$; in other terms, in this case the 3 states fixing the unraveling according to Proposition 1 are even time independent. Remarkably, $\mathbf{R2}_{\psi(t)}$ explicitly demonstrates that the measurement basis can be fixed once and for all, without any state and time dependence.

Unraveling with **R3** and **W**

Finally, we consider the rate operator

$$\mathbf{R3}_\psi = \frac{1}{2}\sum_{k=1}^3 \gamma_k(t)\sigma_k|\psi(t)\rangle\langle\psi(t)|\sigma_k - \frac{1}{2}\gamma_3(t)|\psi(t)\rangle\langle\psi(t)|, \qquad (52)$$

which is positive as shown in Appendix C. The corresponding deterministic evolution is fixed by the linear operator $K3(t) = \frac{i}{4}[\gamma_1(t) + \gamma_2(t)]\mathbb{1}$. We show the simulation results in Fig. 2 (a) and (b). The example realizations in Fig. 2 (a) demonstrate that, similarly to **R1** (cf. Fig. 1), the jumps continue even though the steady state has been reached. However, contrary to **R1**, now it holds all the time that $\rho_{11} \leqslant 0.1$ or $\rho_{11} \geqslant 0.9$. This can be seen more clearly in Fig. 2 (b). While the distribution of trajectories in the steady state for **R1** contained arcs on the western and eastern sides of the XZ-plane of the Bloch sphere, now with **R3** the distribution covers arcs on the northern and southern sides of the circle. As before, there is excellent
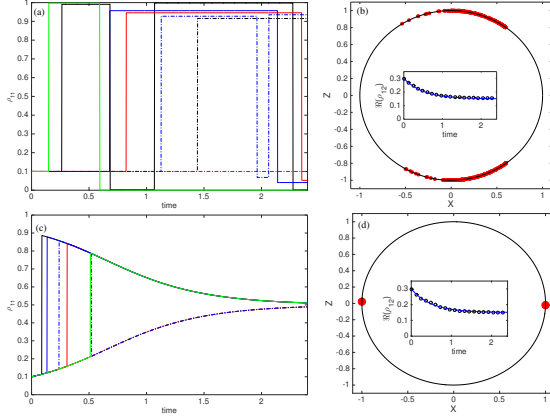
Figure 2: Simulation results using rate operator **R3** [(a), (b)] and **W** [(c), (d)]. Seven example pure state trajectories are displayed in (a) and (c) by plotting the probability of state $|1\rangle$. Final steady state distributions for Bloch vector X and Z components, with 500 trajectories, are shown in (b) and (d). Here, each dot corresponds to a single trajectory. In (d), all the 500 dots have the value $Z = 0$ and $X = -1/2$ or $X = +1/2$, i.e., we have only two distinctively visible dots. The insets in (b) and (d) demonstrate the agreement between the analytical and simulation results by using the coherence ρ_{12} and having 10^4 trajectories. In the insets, the solid line is the analytical result and the dots are the simulation results. The error bars are similar to the size of the dots. In all the panels, the initial state is $|\psi(0)\rangle = \sqrt{0.1}|1\rangle + \sqrt{0.9}|2\rangle$ and the used time step size is $dt = 0.002$.

agreement between the analytical and simulation results [see the inset of Fig. 2 (b).]

The last operator we consider is **W**, see Eq. (12). We display the simulation results in Fig. 2 (c) and (d). With the example realizations in Fig. 2 (c), one can clearly see that now also the deterministic evolution changes the states. Moreover, the jumps happen between a pair of states only and terminate when the steady state is reached. Fig. 2 (d) shows that similarly to **R2** [cf. Fig. 1 (d)], all the trajectories eventually end up being on one of two states on the equator of the Bloch sphere. However, how they reach these points is totally different with respect to **R2**. In terms of the measurement scheme, there is another crucial difference between **W** and **R2**. With **W** the post-measurement states are time dependent, while with **R2** they are time independent.

Table 1 collects and compares the properties of all the used four operators in terms of (i) whether the quantum jumps continue also in the asymptotic regime or terminate when the steady state is reached, (ii) whether the deterministic evolution changes the state of the trajectories, (iii) whether the post-measurement states are time dependent or time independent, and (iv) what is the effective ensemble size in the simulation
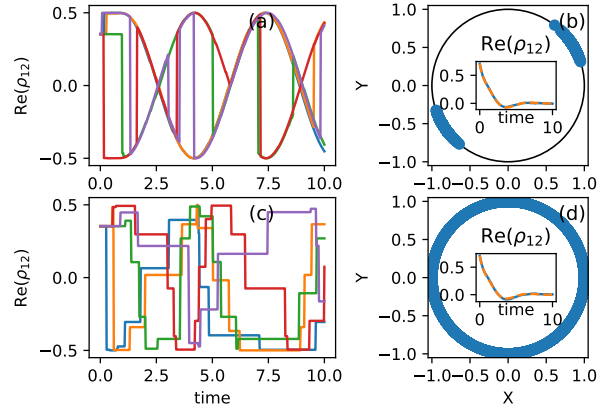

Figure 3: Simulation results using rate operator **R1** [(a), (b)] and **R1**$'$ [(c), (d)] for the model (48) with time dependent driving. Example trajectories are displayed in (a) and (c). Final steady state distributions for Bloch vector X and Y components are shown in (b) and (d). The insets in (b) and (d) demonstrate the agreement between the analytical results (solid line) and simulation results (dots), with 10^4 trajectories.

(how many different kinds of state vectors the ensemble consists of point-wise in time). Overall, the rate operator **R2** has the most appealing properties from simulation and fundamental interpretation points of views.

5.2 Driven master equation

As a second example, we add a time-dependent driving $b(t)$ to the evolution (48) and consider the decay rates $\gamma_1 = \gamma_2 = 1$ and $\gamma_3(t) = -\frac{1}{2}\tanh t$. For the driving, we choose

$$b(t) = C + \int_0^t ds\, \Omega(s; \mu, \sigma) \qquad (53)$$

including an integral over the Gaussian function

$$\Omega(s; \mu, \sigma) = \frac{1}{\sqrt{2\pi}\sigma} e^{-(s-\mu)^2/(2\sigma^2)}$$

and a constant

$$C = \int_{-\infty}^0 ds\, \Omega(s; \mu, \sigma).$$

At time $t = 0$, $b(0) = C$ and $b(t) \to 1$ when $t \gg (\mu + \sigma)$; the amplitude of the drive is ramped up from the initial value C to the asymptotic value 1 over a time-scale fixed by σ, essentially modeling a finite time quench of the Hamiltonian for the open system. The driving does not affect the positivity of the rate operators **R1** and **R2**. However, we use the decomposition (3) and define a new

Rate operator	Asymptotic jumps?	Deterministic changes?	Time-independent post-measurement states?	Effective ensemble size
R1	yes	no	no	∞
R2	no	no	yes	3
R3	yes	no	no	∞
W	no	yes	no	2

Table 1: The basic characterization of the four used rate operators for stochastic simulations. Quantum jumps can either continue or terminate when steady state is reached. Depending on the form of the effective Hamiltonian giving the deterministic evolution, the state of the trajectory can either change or remain unchanged after renormalization. The states after the measurements in the continuous-measurement scheme can be either time dependent or time independent. The effective ensemble size describes how many different kinds of state vectors the ensemble consists of point-wise in time.

rate operator

$$\mathbf{R1'}_{\psi(t)} = \mathbf{R1}_{\psi(t)} + i\frac{b(t)}{2}[\sigma_z, |\psi(t)\rangle\langle\psi(t)|], \quad (54)$$

which fully takes into account the driving, so that the deterministic evolution between the jumps will not depend on it. In other terms, as announced earlier, we can implement the simulation of time-dependent coherent driving with pure jump dynamics (provided that the rate operator $\mathbf{R1'}$ is positive).

In Fig. 3 we plot the dynamics for $\mu = 1$, $\sigma = 1/4$ and for an initial state $|\psi_0\rangle = \cos\frac{\pi}{8}|1\rangle + \sin\frac{\pi}{8}|2\rangle$. In panel (a) the coherent driving is clearly visible in the deterministic evolution between the jumps when using the rate operator $\mathbf{R1}$. In contrast, in panel (c) the sample trajectories do not have any deterministic evolution between the jumps since the driving is absorbed by the rate operator $\mathbf{R1'}$. In the insets of panels (b) and (d), we verify that we indeed unravel the dynamics of Eq. (48). The distribution of the states in the long time limit can be understood by looking at $\varphi(t) = \arctan\frac{y(t)}{x(t)}$, i.e., the angle between the x- and y-axis of the Bloch sphere, measured from the positive x-axis. In the long time limit, when $b(t) \approx 1$ and all of the trajectories have almost reached the equator of the Bloch sphere, each jump just shifts the phase $\varphi(t_+) = \varphi(t_-) \pm \frac{\pi}{4}$, where times $t_\pm$ are just after and before the jump, respectively. The initial transient period randomizes the phases and the resulting smeared distribution for the phase, as seen in panel (d) of Fig. 3, occurs.

For further confirmation, we plot in Figure 4 $\varphi(t)$ for a single trajectory. We clearly see that after a transient period the phase changes during the jumps in steps $\frac{\pi}{4}$, which can be understood as follows. Let $z^2 = \cos^2\theta$ be the squared z-component of a unit Bloch vector in spherical coordinates. The rate operators $\mathbf{R1}$ and $\mathbf{R1'}$ both induce a map $z^2 \mapsto \frac{\alpha^2 z^2}{(2-\alpha)^2}$ when $t \to \infty$. Hence, the jumps push the dynamics on the equatorial plane of
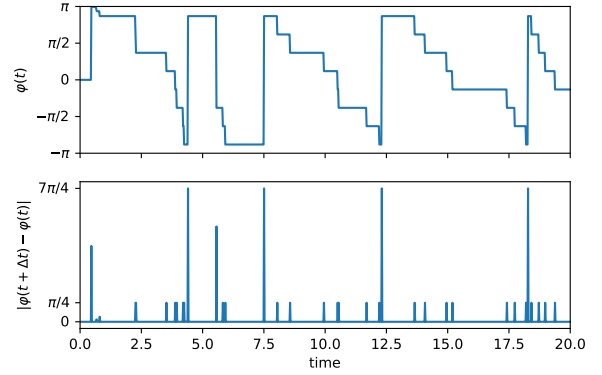

Figure 4: The phase evolution (upper panel) and phase jumps (lower panel) for a single trajectory with time dependent driving. We can see that initially there is a transient where the phase jumps are not multiples of $\pi/4$. This leads to the smearing of the ensemble in the long time limit observed in Fig. 3

.

the Bloch sphere. Since the coherent driving preserves the z-component, the pure states of the ensemble will be distributed along the equator of the Bloch sphere in the long time limit. Any such pure state can be written as $|\psi\rangle = \frac{1}{\sqrt{2}}(|1\rangle + e^{i\varphi}|2\rangle)$. The eigenstates of the rate operator $\mathbf{R1'}_\psi$ in the long time limit are $|\phi_{\psi,\pm}\rangle = \frac{1}{2}(|1\rangle \pm e^{-i\varphi}\xi|2\rangle)$, where $\xi = \frac{1+ib}{\sqrt{1+b^2}}$. Importantly, $|\xi| = 1$ and the relative phase of the eigenstates is $e^{i\varphi}\xi$. In the long time limit, the effect of the quantum jumps corresponds to phase jumps $e^{i\phi} \mapsto \pm e^{i\phi}\xi$. In the long time limit $b(t) = 1$. Interestingly, the phase jumps for the rate operator $\mathbf{R1'}$ in the special case $b = 1$ are rational multiples of π in the long time limit. Namely, $\xi = e^{i\pi/4}$ which is the 8th root of unity.

In Fig. 5 we plot the dynamics for time-independent driving $b(t) = 1$ and especially in panel d) we can see how in this case the definite phase relations are
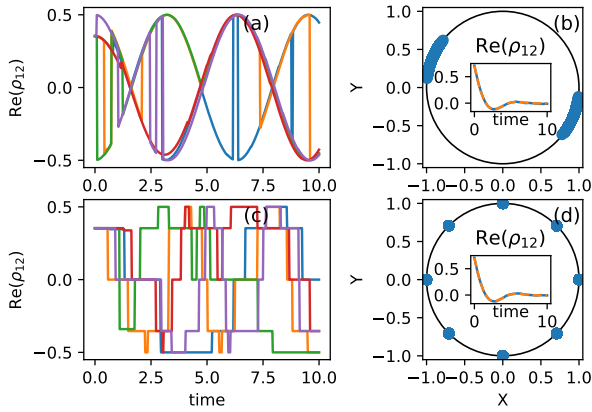
Figure 5: Time independent driving for $b(t) = 1$. In panel a) we plot the dynamics using rate operator **R1** and the driving term is clearly visible in the real part of the coherences. In panel b) we verify in the inset the validity with the simulations and plot the distribution of Bloch vectors in the ensemble at at the final time. In paneld c) we use the rate operator **R1'** and the trajectories contain only jumps. In panel d) we plot the Bloch vectors of the ensemble at the final time. Clearly, the phase is rational multiple of $\pi/4$ for every member of the ensemble.

preserved. The phase $\varphi(t)$ aquires values which are rational multiples of $\pi/4$ for every trajectory of the ensemble.

6 Conclusions

We introduced a class of quantum-jump unravelings (denoted as **R**-ROQJ) that interpolates between MCWF for CP-divisible dynamics and the rate-operator unraveling for P-divisible evolutions [35,51]. **R**-ROQJ guarantees a well-defined continuous-measurement scheme for the class of quantum evolutions defined by the dissipativity condition (46), which is strictly stronger than P-divisibility. Furthermore, **R**-ROQJ takes full advantage of the freedom one has in dividing the master equation into a determinisitic and a jump part, by setting a desired time-independent linear non-Hermitian Hamiltonian, even in the case of an external driving, or selecting a fixed post-jump basis.

The approach put forward here will likely be useful also to deal with more general classes of non-Markovian dynamics, by including reversed jumps in the unraveling [30,31]. In [35], reversed jumps for the standard ROQJ were defined, thus showing that they can be integrated effectively with ROQJ. Even more, the combination of reversed jumps and **R**-ROQJ will allow us to fully exploit the freedom in manipulating the deterministic and jump parts of the unraveling, without having to

restrict to rate operators with positive eigenvalues.

Taking into account more complex, higher dimensional open-system dynamics, it will be possible to perform a detailed comparison of the efficiency of our method with respect not only to different jump-based unravelings, but also to other techniques to solve general master equations. In addition, the definition of different unravelings based on distinct master-equation representations associated with the very same dynamics might lead to novel insights to connect the jumpless part of the evolution of an open quantum system to effective non-Hermitian Hamiltonians and their engineering [64–69]. Finally, in future work we will consider the diffusive limit of **R**-ROQJ unravelings; with a similar approach as in Ref. [17], we could interpolate between piecewise deterministic and continuous quantum trajectories for the **R**-ROQJ, and also between the ROQJ quantum trajectory descriptions presented in [35,51]

Acknowledgments

References

[1] H.-P. Breuer and F. Petruccione, *The Theory of Open Quantum Systems* (Oxford Univ. Press, Oxford, 2007).

[2] H.J. Carmichael,*An Open System Approach to Quantum Optics*, Lectures Notes in Physics (Springer, Berlin, 1993).

[3] J. Dalibard, Y. Castin, and K. Mølmer, Phys. Rev. Lett. **68**, 580 (1992).

[4] T. Basche, S. Kummer, and C. Brauchle, Nature **373**, 132 (1995).

[5] S. Peil and G. Gabrielse, Phys. Rev. Lett. **83**, 1287 (1999).

[6] F. Jelezko, I. Popa, A. Gruber, C. Tietz, J. Wrachtrup, A. Nizovtsev, and S. Kilin, Appl. Phys. Lett. **81**, 2160 (2002).

[7] S. Gleyzes, S. Kuhr, C. Guerlin, J. Bernu, S. Deléglise, U.B. Hoff, M. Brune, J.-M. Raimond, and S. Haroche, Nature **446**, 297 (2007).

[8] R. Vijay, D. H. Slichter, and I. Siddiqi, Phys. Rev. Lett. **106**, 110502 (2011).

[9] Z. K. Minev, S. O. Mundhada, S. Shankar, P. Reinhold, R. Gutiérrez-Jáuregui, R.J. Schoelkopf, M. Mirrahimi, H. J. Carmichael, and M.H. Devoret, Nature **570**, 200 (2019).

[10] M. B. Plenio and P. L. Knight, Rev. Mod. Phys. **70**, 101 (1998).

[11] A.J. Daley, Adv. Phys. **63**, 77 (2014).

[12] I.Percival, *Quantum State Diffusion* (Cambridge University Press, Cambridge, England, 2002)

[13] A. Barchielli and M. Gregoratti, *Quantum Trajectories and Measurements in Continuous Time: The Diffusive Case*, Lecture Notes in Physics 782 (Springer, Berlin, 2009).

[14] H.M. Wiseman and G.J. Milburn, Phys. Rev. A **47**, 1652 (1993).

[15] W. T. Strunz, L. Diósi, and N. Gisin, Phys. Rev. Lett. **82**, 1801 (1999).

[16] T. Yu, L. Diósi, N. Gisin, and W. T. Strunz, Phys. Rev. A **60**, 91 (1999).

[17] K. Luoma, W.T. Strunz, and J. Piilo, Phys. Rev. Lett. **125**, 150403 (2020).

[18] K. W. Murch, S. J. Weber, C. Macklin, and I. Siddiqi, Nature **502**, 211 (2013).

[19] P. Campagne-Ibarcq, P. Six, L. Bretheau, A. Sarlette, M. Mirrahimi, P. Rouchon, and B. Huard, Phys. Rev. X **6**, 011002 (2016).

[20] S. Hacohen-Gourgy, L.S. Martin, E. Flurin, V.V. Ramasesh, K.B. Whaley, and I. Siddiqi, Nature **538**, 491 (2016).

[21] Q. Ficheux, S. Jezouin, Z. Leghtas, and B. Huard, Nat. Comm. **9**, 1926 (2018).

[22] A. Barchielli and V.P. Belavkin, J. Phys. A: Math. Gen. **24**, 1495 (1991).

[23] E.-M. Laine, J. Piilo, and H.-P. Breuer, Phys. Rev. A **81**, 062115 (2010).

[24] D. Chruscinski, A. Kossakowski, and Á. Rivas, Phys. Rev. A **83**, 052128 (2011).

[25] Á. Rivas and S. F. Huelga, *Open Quantum Systems* (Springer, New York, 2012).

[26] Á. Rivas, S. F. Huelga, and M. B. Plenio, Phys. Rev. Lett. **105**, 050403 (2010).

[27] Á. Rivas, S. F. Huelga, and M. B. Plenio, Rep. Prog. Phys. **77**, 094001 (2014).

[28] H.-P. Breuer, E.-M. Laine, and J. Piilo, Phys. Rev. Lett. **103**, 210401 (2009).

[29] H.-P. Breuer, E.-M. Laine, J. Piilo, and B. Vacchini, Rev. Mod. Phys. **88**, 021002 (2016).

[30] J. Piilo, S. Maniscalco, K. Härkönen, and K.A. Suominen, Phys. Rev. Lett. **100**, 180402 (2008).

[31] J. Piilo, K. Härkönen, S. Maniscalco, and K.A. Suominen, Phys. Rev. A **79**, 062112 (2009).

[32] J. Gambetta and H.M. Wiseman, Phys. Rev. A **68**, 062104 (2003).

[33] L. Diósi, Phys. Rev. Lett. **100**, 080401 (2008).

[34] H.M. Wiseman and J.M. Gambetta, Phys. Rev. Lett. **101**, 140401 (2008).

[35] A. Smirne, M. Caiaffa, and J. Piilo, Phys. Rev. Lett. **124**, 190402 (2020).

[36] L. Diósi, Phys. Lett. A **112**, 288 (1985).

[37] L. Diósi, Phys. Lett. A **114**, 451 (1986).

[38] L. Diósi, J. Phys. A **21**, 2885 (1988).

[39] N. Gisin, Helv. Phys. Acta **63**, 929 (1990).

[40] B. Vacchini, A. Smirne, E.-M. Laine, J. Piilo, H.P. Breuer, New J. Phys. **13**, 093004 (2011).

[41] D. Chruściński and S. Maniscalco, Phys. Rev. Lett. **112**, 120404 (2014).

[42] S. Wißmann, H.-P. Breuer, B. Vacchini, Phys. Rev. A **92**, 042108 (2015).

[43] H. M. Wiseman and G. J. Milburn, *Quantum Measurement and Control* (CUP, Cambridge, 2010).

[44] J. Zhangab, Y.-X. Liu, R.-B. Wuab, K. Jacobs, and F. Nori, Phys. Rep. **679**, 1 (2017).

[45] S. Hacohen-Gourgy, L. P. Garcìa-Pintos, L.S. Martin, J. Dressel, and I. Siddiqi, Phys. Rev. Lett. **120**, 020505 (2018).

[46] L.S. Martin, W.P. Livingston, S. Hacohen-Gourgy, H.M. Wiseman and I. Siddiqi, Nat. Phys. **16**, 1046 (2020).

[47] L. Magrini, P. Rosenzweig, C. Bach, A. Deutschmann-Olek, S.G. Hofer, S. Hong, N. Kiesel, A. Kugi, and M. Aspelmeyer, Nature **595**, 373 (2021).

[48] G. Lindblad, Comm. Math. Phys. **48**, 119 (1976).

[49] V. Gorini, A. Kossakowski, and E.C.G. Sudarshan, J. Math. Phys. **17**, 821 (1976).

[50] D. Chruscinski, and A. Kossakowski, Phys. Rev. Lett. **104**, 070406 (2010).

[51] M. Caiaffa, A. Smirne, and A. Bassi, Phys. Rev. A **95**, 062101 (2017).

[52] T.A. Brun, Phys. Rev. A **61**, 042107 (2000).

[53] T.A. Brun, Am. J. Phys. **70**, 719 (2002).

[54] L. Diósi, J.Phys. A **50**, 16LT01 (2017).

[55] M.J.W. Hall, J.D. Cresser, L. Li, and E. Andersson, Phys. Rev. A **89**, 042120 (2014).

[56] D. Chruściński and F.A. Wudarski, Phys. Rev. A **91**, 012104 (2015).

[57] N. Megier, D. Chruscinski, J. Piilo, and W.T. Strunz, Sci. Rep. **7**, 6379 (2017).

[58] T. Heinosaari and M. Ziman, *The Mathematical Language of Quantum Theory*, (Cambridge University Press, Cambridge, 2012).

[59] H.M. Wiseman, Quantum Semiclass. Opt. **8**, 205 (1996).

[60] V. Paulsen, *Completely Bounded Maps and Operator Algebras* (Cambridge University Press, Cambridge, 2003).

[61] E. Størmer, *Positive Linear Maps of Operator Algebras*, Springer Monographs in Mathematics (Springer, New York, 2013).

[62] K. Mølmer and Y. Castin, Quantum Semiclass. Opt. **8**, 49 (1996).

[63] D. Chruściński and F. Mukhamedov, Phys. Rev. A **100**, 052120 (2019).

[64] M. Naghiloo, M. Abbasi, Yogesh N. Joglekar, and K. W. Murch, Nat. Phys. **15**, 1232 (2019).

[65] F. Minganti, A. Miranowicz, R. W. Chhajlany, and F. Nori, Phys. Rev. A **100**, 062131 (2019).

[66] F. Minganti, A. Miranowicz, R. W. Chhajlany, I. I. Arkhipov, and F. Nori, Phys. Rev. A **101**, 062112 (2020).

[67] Y. Ashida, Z. Gong, and M. Ueda, Adv. Phys. **69**, 3 (2020).

[68] W. Chen, M. Abbasi, Y. N. Joglekar, and K. W. Murch, Phys. Rev. Lett. **127**, 140504 (2021).

[69] F. Roccati, G.M. Palma, F. Bagarello, and F. Ciccarello Op. Syst. Inf. Dyn. **29**, 2250004 (2022).

A Proof of Proposition 1

Consider $\mathcal{H}_S = \mathbb{C}^2$ and a master equation as in Eq.(1); moreover assume that there is a basis $\{|\varphi_1\rangle, |\varphi_2\rangle\}$ and a linear operator $\mathbf{C}(t)$ on $\mathbb{C}^2$ such that Eqs.(39) and (42) hold. First note that Eq.(39), along with the Hermiticity preservation condition, imply (we neglect from now on the time dependence) $J_{ij}^{kl} = J_{ji}^{lk}$. Using the latter, it is readily shown that the action of $\mathcal{J}_t'$ in Eq.(3) with $\mathbf{C}$ defined as in Eq.(40) can be written as

$$\mathcal{J}_t'(\overline{\rho}) = \mathcal{J}_t(\overline{\rho}) + \frac{1}{2}\left(\mathbf{C}\overline{\rho} + \overline{\rho}\mathbf{C}^\dagger\right) = \begin{pmatrix} \alpha & \beta \\ \beta & \alpha \end{pmatrix} \quad \begin{cases} \alpha = & (2J_{11}^{12} + y)\rho_{12} + J_{11}^{22}\rho_{22} + J_{22}^{11}\rho_{11} \\ \beta = & (J_{12}^{11} + \frac{y}{2} + J_{11}^{12} + J_{22}^{12})\rho_{11} + (J_{12}^{22} + \frac{y}{2})\rho_{22} \\ & + \frac{1}{2}(2J_{12}^{12} + 2J_{12}^{21} + J_{22}^{11} - J_{11}^{11} + J_{11}^{22} - J_{22}^{22})\rho_{12} \end{cases} \tag{A.1}$$

for any state $\overline{\rho}$ such that

$$\rho_{12} = \rho_{21}, \tag{A.2}$$

where indeed $\rho_{ij} = \langle\varphi_i|\overline{\rho}|\varphi_j\rangle$ (i.e., there are no phases with respect to the selected basis).

Now, the crucial observation is that the matrix in Eq.(A.1) has *fixed* eigenvectors: for any values of α and β, they are in fact given by

$$|\varphi_\pm\rangle = \frac{1}{\sqrt{2}}\left(|\varphi_1\rangle \pm |\varphi_2\rangle\right), \tag{A.3}$$

which directly implies the statement to be proven, whenever the rate operator is positive if referred to pure states satisfying Eq.(A.2):

- as said, we choose an initial state $|\psi_0\rangle$ that satisfies Eq.(41);

- but then, due to Eq.(42), the state $|\psi_0(t_1)\rangle$ before the first jump at time t_1 (recall that $D(t, s)$ is defined in Eq.(43))

$$\frac{D(t_1, 0)|\psi_0\rangle}{\|D(t_1, 0)|\psi_0\rangle\|}$$

will be such that Eq.(A.2) holds, so that the jump operator $\mathbf{R}_{\psi_0(t_1)} = \mathcal{J}_t'(|\psi_0(t_1)\rangle\langle\psi_0(t_1)|)$ fixed by Eq.(3) with $\mathbf{C}(t)$ as in Eq.(40) has the two eigenvectors $|\varphi_\pm\rangle$ in Eq.(A.3);

- thus, after the jump (that is well defined due to the positivity of the rate operator) the system will be either in $|\varphi_+\rangle$ or in $|\varphi_-\rangle$;

- since also the latter are in the form as in Eq.(41) the state before the second jump,

$$\frac{D(t_2, t_1) |\varphi_\pm\rangle}{\|D(t_2, t_1) |\varphi_\pm\rangle\|},$$

will still satisfy Eq.(A.2), so that the state after the second jump will be either $|\varphi_+\rangle$ or $|\varphi_-\rangle$, and so on.

All in all, we have the 3 possible families of states $\{|\psi_0(t)\rangle, |\varphi_+(t,s)\rangle, |\varphi_-(t,s)\rangle\}$ that are obtained from $\{|\psi_0\rangle, |\varphi_+\rangle, |\varphi_-\rangle)\}$ via the deterministic evolution in Eq.(43); the instants of occurrence of the jumps will determine which parts of the deterministic evolution will be actually involved in each trajectory.

B Proof of Proposition 3

Defining

$$\mathbf{K}(t) = \int_{U(N)} \mathcal{L}_t^\dagger(U^\dagger)U dU, \tag{B.1}$$

one finds for an arbitrary $V \in U(N)$

$$\int_{U(N)} \mathcal{L}_t^\dagger(VU^\dagger)U dU = \int_{U(N)} \mathcal{L}_t^\dagger(U'^\dagger)U'V dU' = \mathbf{K}(t)V, \tag{B.2}$$

with $U' = UV^\dagger$. Hence for an arbitrary system operator X one has

$$\int_{U(N)} \mathcal{L}_t^\dagger(XU^\dagger)U dU = \mathbf{K}(t)X. \tag{B.3}$$

Now we use the dissipativity condition, Eq.(46),

$$\mathcal{L}_t^\dagger(Y^\dagger Y) \geq \mathcal{L}_t^\dagger(Y^\dagger)Y + Y^\dagger \mathcal{L}_t^\dagger(Y), \tag{B.4}$$

for $Y = UX$, with $U \in U(N)$. It leads to

$$\mathcal{L}_t^\dagger(Y^\dagger Y) \geq \mathcal{L}_t^\dagger(X^\dagger U^\dagger)UX + X^\dagger U^\dagger \mathcal{L}_t^\dagger(UX) = \mathcal{L}_t^\dagger(X^\dagger U^\dagger)UX + X^\dagger[\mathcal{L}_t^\dagger(X^\dagger U^\dagger)U]^\dagger. \tag{B.5}$$

Averaging over $U(N)$ yields

$$\int_{U(N)} \mathcal{L}_t^\dagger(Y^\dagger Y)dU \geq \int_{U(N)} \mathcal{L}_t^\dagger(X^\dagger U^\dagger)U dU\, X + +X^\dagger \left(\int_{U(N)} \mathcal{L}_t^\dagger(X^\dagger U^\dagger)U DU\right)^\dagger = \mathbf{K}(t)X^\dagger X + X^\dagger X\mathbf{K}^\dagger(t) \tag{B.6}$$

and hence defining a linear map as

$$\mathbf{J}_t^\dagger(X) = \mathcal{L}_t^\dagger(X) - (\mathbf{K}(t)X + X\mathbf{K}^\dagger(t)), \tag{B.7}$$

we have shown that

$$\mathbf{J}_t^\dagger(X^\dagger X) \geq 0, \tag{B.8}$$

which proves that the map $\mathbf{J}_t$ is positive.

C   Positivity of the rate operators $\mathbf{R1}_{\psi(t)}$, $\mathbf{R2}_{\psi(t)}$ and $\mathbf{R3}_{\psi(t)}$

Here, we prove the positivity of $\mathbf{R1}_{\psi(t)}$, $\mathbf{R2}_{\psi(t)}$, and $\mathbf{R3}_{\psi(t)}$ defined in Sec.5, fixed by Eqs.(50), (51) and (52), assuming only that the $\gamma_k(t)$ satisfy P-divisibility condition, that is, $\gamma_i(t) + \gamma_j(t) \geq 0$ for $i \neq j = 1, 2, 3$ and that $\gamma_3(t) < 0$, so that P-divisibility means that

$$\gamma_k(t) + \gamma_3(t) \geq 0 \ , \ \ k = 1, 2.$$

Note that the eternal non-Markovian dynamics considered in the main text is a special case of this class of dynamics.

First, we note that the qubit generator

$$\mathcal{L}_t(\rho) = \frac{1}{2} \sum_{k=1}^{3} \gamma_k(t)(\sigma_k \rho \sigma_k - \rho), \tag{C.1}$$

may be rewritten as

$$\mathcal{L}_t(\rho) = \sum_{k=1}^{3} \gamma_k(t)(J_k(\rho) - \rho), \tag{C.2}$$

where

$$J_k(\rho) = \frac{1}{2}(\sigma_k \rho \sigma_k + \rho), \tag{C.3}$$

are CPTP for $k = 1, 2, 3$. We then have the following result.

Proposition 4. *The map (cf. Eq. (50))*

$$\mathbf{J}_t(\rho) = \sum_{k=1}^{3} \gamma_k(t) J_k(\rho) = \mathcal{J}_t(\rho) + \frac{\gamma(t)}{2}\rho \tag{C.4}$$

is positive.

The proof is based on the following observation: for a qubit system a linear map $\Phi : M_2(\mathbb{C}) \to M_2(\mathbb{C})$ is positive if and only the corresponding Choi matrix C_Φ

$$C_\Phi := \sum_{i,j=1}^{2} |i\rangle\langle j| \otimes \Phi(|i\rangle\langle j|)$$

satisfies

$$C_\Phi = A + (\mathbb{1} \otimes T)B,$$

where A and B are positive 4×4 matrices, and '$\mathbb{1} \otimes T$' denotes partial transposition. The Choi matrix for the map $\mathbf{J}_t$ reads

$$C_{\mathbf{J}_t} = \left(\begin{array}{cc|cc} \gamma_1 + \gamma_2 + 2\gamma_3 & 0 & 0 & \gamma_1 + \gamma_2 \\ 0 & \gamma_1 + \gamma_2 & \gamma_1 - \gamma_2 & 0 \\ \hline 0 & \gamma_1 - \gamma_2 & \gamma_1 + \gamma_2 & 0 \\ \gamma_1 + \gamma_2 & 0 & 0 & \gamma_1 + \gamma_2 + 2\gamma_3 \end{array} \right), \tag{C.5}$$

where we skipped the time dependence. Note, that $C_{\mathbf{J}_t} = A + (\mathbb{1} \otimes T)B$, where

$$A = \left(\begin{array}{cc|cc} \gamma_1 + \gamma_2 + 2\gamma_3 & 0 & 0 & \gamma_1 + \gamma_2 + 2\gamma_3 \\ 0 & \gamma_1 + \gamma_2 + 2\gamma_3 & \gamma_1 - \gamma_2 & 0 \\ \hline 0 & \gamma_1 - \gamma_2 & \gamma_1 + \gamma_2 + 2\gamma_3 & 0 \\ \gamma_1 + \gamma_2 + 2\gamma_3 & 0 & 0 & \gamma_1 + \gamma_2 + 2\gamma_3 \end{array} \right), \tag{C.6}$$

and

$$B = -2\gamma_3 \begin{pmatrix} 0 & 0 & 0 & 0 \\ 0 & 1 & 1 & 0 \\ \hline 0 & 1 & 1 & 0 \\ 0 & 0 & 0 & 0 \end{pmatrix}. \tag{C.7}$$

Since $\gamma_3(t) < 0$ one has $B \geq 0$. Now, $A \geq 0$ if and only if

$$\gamma_1 + \gamma_2 + 2\gamma_3 \geq |\gamma_1 - \gamma_2|. \tag{C.8}$$

Let us consider two scenario:

1. if $\gamma_1 \geq \gamma_2$, then (C.8) is equivalent to $\gamma_2 + \gamma_3 \geq 0$,

2. conversely, if $\gamma_2 \geq \gamma_1$, then (C.8) is equivalent to $\gamma_1 + \gamma_3 \geq 0$,

which ends the proof of positivity of A. Now, since A and B are positive, the map $\mathbf{J}_t$ is positive and hence $\mathbf{R1}_{\psi(t)} \geq 0$.

Positivity of $\mathbf{R2}_{\psi(t)}$ is evident due to the relation

$$\mathbf{R2}_{\psi(t)} = \mathbf{R1}_{\psi(t)} - \gamma_3(t)|\psi(t)\rangle\langle\psi(t)|, \tag{C.9}$$

and $\gamma_3(t) < 0$. Finally, the operator $\mathbf{R3}_{\psi(t)}$ corresponds to the map $\frac{1}{2}(\sum_k \gamma_k \sigma_k \rho \sigma_k - \gamma_3\rho)$. Its Choi matrix reads

$$C = \begin{pmatrix} 0 & 0 & 0 & -2\gamma_3 \\ 0 & \gamma_1 + \gamma_2 & \gamma_1 - \gamma_2 & 0 \\ \hline 0 & \gamma_1 - \gamma_2 & \gamma_1 + \gamma_2 & 0 \\ -2\gamma_3 & 0 & 0 & 0 \end{pmatrix} = A' + (\mathbb{1} \otimes T)B', \tag{C.10}$$

where

$$A' = \begin{pmatrix} 0 & 0 & 0 & 0 \\ 0 & \gamma_1 + \gamma_2 + 2\gamma_3 & \gamma_1 - \gamma_2 & 0 \\ \hline 0 & \gamma_1 - \gamma_2 & \gamma_1 + \gamma_2 + 2\gamma_3 & 0 \\ 0 & 0 & 0 & 0 \end{pmatrix}, \tag{C.11}$$

and $B' = B$ defined by (C.7). The proof of positivity of A' is very similar to that of A.

D Fixed post-jump states for the eternal non-Markovian dynamics

Here, we first show explicitly that the dynamics defined by the master equation (48) is actually a special case of the two-level system dynamics identified by Prop.1, so that we can define a $\mathbf{R}$-ROQJ unraveling with fixed post-jump states via Eq.(40). We will then discuss the positivity of such an unraveling.

Consider the basis $\{|1\rangle, |0\rangle\}$ of eigenvectors of σ_z; in such a basis the coefficients of $\mathcal{J}_t$ according to Eq.(38) read

$$
\begin{pmatrix}
J_{11}^{11}(t) & \gamma_3(t)/2 \\
J_{10}^{11}(t) & 0 \\
J_{01}^{11}(t) & 0 \\
J_{00}^{11}(t) & (\gamma_1(t) + \gamma_2(t))/2 \\
J_{11}^{10}(t) & 0 \\
J_{10}^{10}(t) & -\gamma_3(t)/2 \\
J_{01}^{10}(t) & (\gamma_1(t) - \gamma_2(t))/2 \\
J_{00}^{10}(t) & 0 \\
J_{11}^{01}(t) & 0 \\
J_{10}^{01}(t) & (\gamma_1(t) - \gamma_2(t))/2 \\
J_{01}^{01}(t) & -\gamma_3(t)/2 \\
J_{00}^{01}(t) & 0 \\
J_{11}^{00}(t) & (\gamma_1(t) + \gamma_2(t))/2 \\
J_{10}^{00}(t) & 0 \\
J_{01}^{00}(t) & 0 \\
J_{00}^{00}(t) & \gamma_3(t)/2
\end{pmatrix}
\tag{D.1}
$$

and hence (setting $x = 0$) the operator $\mathbf{C}(t)$ as in Eq.(40) is

$$
\mathbf{C}(t) = \begin{pmatrix} \frac{\gamma_1(t) + \gamma_2(t) - \gamma_3(t)}{2} & y(t) \\ y(t) & \frac{\gamma_1(t) + \gamma_2(t) - \gamma_3(t)}{2} \end{pmatrix} = \frac{\gamma_1(t) + \gamma_2(t) - \gamma_3(t)}{2} \mathbb{1} + y(t)\sigma_x;
\tag{D.2}
$$

while the operator fixing the deterministic evolution according to Eq.(43) is

$$
D(t, s) = \exp\left(-\frac{1}{2} \int_s^t d\tau (\gamma_1(\tau) + \gamma_2(\tau)) \mathbb{1} + y(\tau)\sigma_x\right);
\tag{D.3}
$$

note that for $y(t) = 0$ we recover the rate operator $\mathbf{R2}_{\psi(t)}$ defined by Eq.(51). It is easy to see that the assumptions of Prop.1 in Eq.(39) and (42) hold, so that, starting from an initial state as in Eq.(41), the $\mathbf{R}$-ROQJ fixed by $\mathbf{C}(t)$ as in Eq.(D.2) consists of jumps among 3 deterministically evolving states, whenever the positivity of the rate operator is ensured. In particular, for a continuous family of $\mathbf{R}$-ROQJ this is the case whenever the dynamics is P-divisible, as shown below.

First, recall that the P-divisibility condition for the eternal non-Markovian dynamics is $\gamma_1(t), \gamma_2(t) \geq |\gamma_3(t)|$ for all $t \geq 0$. Moreover, going back to the proof of Prop. 1 in Sec.B, the positivity of the rate operator is fixed by the eigenvalues

$$
\alpha(t) \pm \beta(t)
$$

of $\mathcal{J}_t'(|\psi(t)\rangle \langle\psi(t)|)$, see the first equality in Eq.(A.1). Actually, rather than studying the eigenvalues, it is convenient to look at the trace and determinant of the corresponding 2×2 matrix: for any pure state of the form $|\psi\rangle = c|\varphi_1\rangle \pm \sqrt{1 - c^2}|\varphi_2\rangle$ (i.e., as in Eq.(41)) we then have the two conditions

$$
\alpha(t) = \frac{\gamma_1(t) + \gamma_2(t)}{2} \pm c\sqrt{1 - c^2}y(t) \geq 0
$$

$$
\alpha^2(t) - \beta^2(t) = \left(\frac{\gamma_1(t) + \gamma_2(t)}{2} \pm c\sqrt{1 - c^2}y(t)\right)^2 - \left(\frac{y(t)}{2} \pm c\sqrt{1 - c^2}(\gamma_1(t) - \gamma_3(t))\right)^2 \geq 0.
\tag{D.4}
$$

Both inequalities hold for any $-1 \leq c \leq 1$ if $0 \leq y(t) \leq \gamma_1(t) + \frac{1}{2}\gamma_2(t) - \frac{1}{2}\gamma_3(t)$ for all $t \geq 0$. The validity of the first inequality directly follows from the fact that $\gamma_1(t), \gamma_2(t) \geq 0$ and $\gamma_1(t) + \frac{1}{2}\gamma_2(t) - \frac{1}{2}\gamma_3(t) \leq \gamma_1(t) + \gamma_2(t)$ due to P-divisibility and that the maximum value of $|c|\sqrt{1 - c^2}$ for $-1 \leq c \leq 1$ is $1/2$. For the second inequality, let us consider first the case where the term $\pm c$ appearing in it is positive, so that the inequality becomes

$$
\gamma_1(t) + \gamma_2(t) - y(t) \geq 2|c|\sqrt{1 - c^2}(\gamma_1(t) - \gamma_3(t) - y(t))
$$

as $\gamma_1(t) - \gamma_3(t) \geq 0$ due to P-divisibility and we used that $\alpha(t) \geq 0$, as well as $y(t) \geq 0$; but the maximum value with respect to c of the term at the r.h.s. is $\max\{0, \gamma_1(t) - \gamma_3(t) - y(t)\}$, so that the inequality holds for any $y(t) \leq \gamma_1(t) + \gamma_2(t)$ ($\gamma_2(t) \geq -\gamma_3(t)$ due to P-divisibility). Instead, if $\pm c$ is negative the second inequality in (D.4) becomes

$$\frac{\gamma_1(t) + \gamma_2(t)}{2} - |c|\sqrt{1-c^2}y(t) \geq \left| \frac{y(t)}{2} - |c|\sqrt{1-c^2}(\gamma_1(t) - \gamma_3(t)) \right|.$$

If $y(t) \geq 2|c|\sqrt{1-c^2}(\gamma_1(t) - \gamma_3(t))$, we have $\gamma_1(t) + \gamma_2(t) - y(t) \geq 2|c|\sqrt{1-c^2}(y(t) - (\gamma_1(t) - \gamma_3(t)))$, whose r.h.s. maximum value with respect to c is $\max\{0, y(t) - (\gamma_1(t) - \gamma_3(t))\}$ so that the inequality holds for any $-1 \leq c \leq 1$ if $y(t) \leq \gamma_1(t) + \frac{1}{2}\gamma_2(t) - \frac{1}{2}\gamma_3(t)$. If $y(t) < 2|c|\sqrt{1-c^2}(\gamma_1(t) - \gamma_3(t))$, we have $\gamma_1(t) + \gamma_2(t) + y(t) \geq 2|c|\sqrt{1-c^2}(y(t) + (\gamma_1(t) - \gamma_3(t)))$, whose r.h.s. maximum is $\max\{0, y(t) + (\gamma_1(t) - \gamma_3(t))\}$ so that the inequality is ensured by $\gamma_2(t) \geq -\gamma_3(t)$, as well as $\gamma_1(t), \gamma_2(t), y(t) \geq 0$.

In total, for any $y(t)$ such that $0 \leq y(t) \leq \gamma_1(t) + \frac{1}{2}\gamma_2(t) - \frac{1}{2}\gamma_3(t)$ for all $t \geq 0$ the rate operator $\mathbf{R}_\psi = \mathcal{J}'_t(|\psi\rangle\langle\psi|)$ is positive for any $|\psi\rangle = c|\varphi_1\rangle \pm \sqrt{1-c^2}|\varphi_2\rangle$ with $-1 \leq c \leq 1$ and then if the initial state satisfies the latter condition (which is preserved by the deterministic evolution in Eq.(D.3)), we will have a *positive* rate-operator unravelling with the states $\{|\psi_0(t)\rangle, |\varphi_+(t,s)\rangle, |\varphi_-(t,s)\rangle\}$.